Influence of Extrusion and Digestion on the Nanostructure of High-Amylose Maize Starch

Amparo Lopez-Rubio,*,† Aung Htoon,‡ and Elliot P. Gilbert†

Bragg Institute, Australian Nuclear Science and Technology Organization, PMB 1, Menai, NSW 2234, Australia, and Commonwealth Scientific and Industrial Research Organization, Food Futures National Research Flagship and CSIRO, Food Science Australia, Riverside Corporate Park, North Ryde, NSW, Australia

Received November 27, 2006; Revised Manuscript Received February 17, 2007

An in-depth characterization of the structural changes undergone by high-amylose starch after extrusion and digestion with a pancreatic α-amylase has been carried out. The combination of USAXS, SAXS, XRD, and SEM techniques has provided a wide "picture" of the morphological transformations of starch, covering a length scale from ∼0.3 nm to ∼230 μm. Depending on the extrusion conditions, either gelatinization was attained ("mild" conditions) or single-amylose helix formation was induced ("extreme" conditions). SAXS experiments demonstrated that upon contacting the extruded materials with water, retrogradation took place. A new type of molecular organization with a characteristic repeat length of 5 nm was observed in the dry resistant starch fractions from the extruded high-amylose starch. The crystalline morphology of the resistant starch fractions, as observed by XRD, varied from B-type crystallinity for the "mild" extruded starch to a mixture of C- and V-type crystallinity in the case of "extreme" extrusion.

Introduction

Resistant starch (RS) is the fraction of starch that escapes digestion by α-amylases in the small intestine of healthy individuals. The interest aroused by RS relies in its ability to raise large bowel total short-chain fatty acids, which are correlated with gut health and prevention of several diseases like colorectal cancer.[1] Different types of RS have been established, depending on the starting material.[2] RSIII refers to RS fractions obtained after digestion of processed starch, which is the one of principal interest for industry as most commercial starch products undergo some form of processing before consumption. While the structure of native starches has been widely studied and is quite well characterized, limited information is available about the reorganization of starch after gelatinization and the morphology that makes this fraction of starch resistant to digestion. Understanding the structural mechanisms that allow starch to escape from digestion is of prime importance, since in this way, it will be possible to design and select those processes which render such desirable structural morphologies.

Native starch granules display a quite complex structure with several levels of organization. The two main polymers constituting starch (essentially linear amylose and branched amylopectin) are distributed in amorphous and semicrystalline concentric shells. Some authors propose an intermediate level of organization of these shells in structures named as blocklets.[3] A chiral side chain liquid-crystalline polymeric model has been proposed[4] for the description of the structure and physical properties of starch, where the amylopectin side chains, organized in double helices and constituting the crystalline fraction of starch, are considered as mesogens, attached to the backbone through amorphous and flexible spacer units. The length of these amylopectin double helices seems to be related to the crystalline morphology present (short double helices related to A-type and long double helices to B-type).[5,6] Additional hydrogen bonds are needed to form double helices into crystallites, which provide more protection for the structural elements of the short-range order. Furthermore, the long-range order in native starches is influenced by the water content. Water is, in fact, part of the crystalline unit cell constituting up to 4−7% and 25−27% of A and B polymorphs, respectively.[7−9] An increase in the water content within the granule leads to an increase in the molecular order, as molecular motion and, therefore, chain reorganization is favored.

Heat and humidity involved in many processing conditions lead to the break up of the starch's structure, a phenomenon known as gelatinization, which "erases" the original granule organization. Upon storage of gelatinized starch, the molecules are able to reorganize (recrystallize or retrograde) at temperatures between the glass transition temperature (T_g) and the melting temperature (T_m), and the molecular organization attained during this period is one of the factors which may influence the subsequent resistance to digestion.

Regarding the resistance to digestion of native starches, it has been observed that cereal starches (with A-type crystallinity) are more rapidly hydrolyzed than potato or high-amylose starches (B-type crystallinity). Intuitively, since the packing density of the A polymorph is higher, it might be expected to be more resistant to digestion. However, it has also been noted that in B-type crystalline materials, the amount of crystallinity in their external regions is higher than in the A-type,[10] highlighting that it could be the shell (the structural organization within the granule), instead of the crystal polymorph, responsible for enzyme resistance in native starches (fraction known as RSII). Moreover, native starches, submitted to digestion by pancreatic α-amylase, have shown that the more susceptible or

* Corresponding author. Phone: (61) 2 9717 7273. Fax: (61) 2 97173606. E-mail: amparo.lopez.rubio@ansto.gov.au.
† Australian Nuclear Science and Technology Organization.
‡ Food Science Australia.

10.1021/bm061124s CCC: $37.00 Published 2007 by the American Chemical Society
Published on Web 03/30/2007

"soft" material is preferentially etched, leaving behind the better organized and harder parts of the starch layers.[11] Therefore, it is reasonable to think that by improving the crystallinity, resistance will be increased.

Previous studies on RSIII[12] have concluded that it is composed of essentially linear (1→4)-α-D-glucan chains having a range of chain lengths. It has been suggested that it is mostly the double-helical structure of retrograded amylose that defines this fraction, but depending on the processing conditions and subsequent storage of starch, different structures are obtained, which upon digestion will render different RS morphologies.[13]

Several methods have been studied for improving RS yield such as autoclaving−cooling cycles,[14] acid hydrolysis,[15] and enzymatic debranching,[16] as well as a combination of the previous methods.[17] Applying freeze−thaw cycles has been also observed to accelerate retrogradation of starch,[18] although some of these methods are of doubtful viability from an industrial viewpoint.

Extrusion cooking, on the other hand, is an important method for food processing, especially for starch-based products. It is used for the production of breakfast cereals, pasta, and a huge variety of snacks. Depending on the properties of the raw materials and the process conditions used, final products of great diversity can be obtained. The aim of the present work is to understand the morphological changes undergone by a commercial high-amylose starch upon extrusion at two different conditions and correlate them with the subsequent RSIII structures obtained. These morphologies will also be compared with the structure left after digestion of native starch (RSII).

Experimental Section

Materials. A commercial high-amylose maize starch (~80% amylose content), gelose 80 (Penford Australia Ltd.) was analyzed as received (raw), extruded at two different processing conditions ("mild" → 50% moisture content, 100 °C, and 150 s^{-1} shear rate; "extreme" → 35% moisture content, 140 °C, and 750 s^{-1} shear rate) and after digestion using the method of Muir et al.[19] (kindly supplied by Food Science Australia) to enable investigation of the RS fractions. Briefly, digestion of the starches was carried out at 37 °C during approximately 18 h with pancreatic α-amylase and amyloglucosidase enzyme mixture, and the residue was collected by centrifuging. To minimize the structural changes after the different treatments, all the samples were freeze-dried prior to delivery.

To cover a broader q-range for the study of the nanostructure of starch, a combination of ultrasmall-angle X-ray scattering (USAXS) and small-angle X-ray scattering (SAXS) techniques were used in this work, which provided information in a scale from a few angstroms to few micrometers, i.e., screening over 4 orders of magnitude. USAXS/SAXS experiments were performed both on dry and wet starch. For the latter experiments the starch samples were allowed to equilibrate in excess water for 1 h.

USAXS data were acquired using the USAXS instrument installed at beam line 33ID (XOR-UNI) at the Advanced Photon Source, Argonne National Laboratory, United States. The monochromator was set to 10.99 keV (1.13 Å) generating about 10^{13} photons/s incident on the sample in an area of about 2 mm wide and 0.5 mm high. The USAXS instrument consists of a Bonse−Hart camera using Si 111 artificial channel cut with six reflections prior to the sample as beam conditioning, and similar Si 111 artificial channel cut with six reflections after the sample as analyzer. The instrument uses a photodiode detector with about 9 decades of intensity range between the direct beam and instrument background. USAXS was collected for q-values from 0.00015 to 0.05 $Å^{-1}$, where q is the scattering vector defined as

$$q = \frac{4\pi}{\lambda} \sin \theta$$

where λ is the wavelength and θ is the scattering angle. For these measurements the instrument was set up in slit-smeared geometry, which resulted in slit-smeared data. Data were processed using the code developed for use on this USAXS instrument, including numerical desmearing of the USAXS data using the Lake method[20] and implemented by Long et al.[21]

Small-angle X-ray scattering measurements were performed on a Bruker Nanostar SAXS camera, with pinhole collimation for point focus geometry. The instrument source is a copper rotating anode (0.3 mm filament) operating at 45 kV and 110 mA, fitted with cross-coupled Göbel mirrors, resulting in Cu Kα radiation wavelength of 1.54 Å. The SAXS camera is fitted with a Hi-star 2D detector (effective pixel size 100 μm). The sample-to-detector distance was chosen to be 65 mm which provided a q-range from 0.02 to 0.3 $Å^{-1}$. Some measurements were also conducted with a sample-to-detector distance of 25 mm for observing scattering up to $q \sim 0.75$ $Å^{-1}$. Samples were presented in 2 mm glass capillaries. The optics and sample chamber were under vacuum to minimize air scatter. Scattering files were background subtracted, normalized to sample transmission, and then radially averaged using macros written in the Igor software package (Wavemetrics, Lake Oswego, OR).

X-ray diffraction (XRD) was carried out on a Panalytical X'Pert Pro diffractometer. The instrument was equipped with a Cu long fine focus tube, programmable incident beam divergence slit, and diffracted beam scatter slit (both fixed at 0.125°) and an X'celerator high-speed detector. The samples were examined over the angular range of 2−40° with a step size of 0.0332° and a count time of 800 s per point. Crystallinity determination was carried out using the X'Pert software. This program automatically determines the amorphous hump of the diffraction pattern, and the crystallinity can be easily calculated from the intensity ratio of the diffraction peaks (I_{net}) and of the sum of all intensity measured (I_{total}):

$$\text{crystallinity (\%)} = 100 \times (I_{net}/I_{total})$$

Scanning electron microscopy (SEM) was conducted on a JEOL (JSM-6400) microscope (JEOL, Ltd., Tokyo, Japan) at an accelerating voltage of 15 kV and a working distance down to 14 mm. The dried starch materials before and after processing and digestion were sprayed on circular metal stubs previously covered with double-sided adhesive and coated with carbon. After examination of the samples, different regions depicting interesting morphological features were selected and photographed.

Results and Discussion

Effect of Extrusion on the Structure of High-Amylose Starches. Being aware of the influence that water has on the structural order of starch, USAXS/SAXS experiments were carried out at two different humidity conditions: "dry" (without adding any water) and in excess water.

In Figure 1, the combined USAXS/SAXS curves for the native, "mild", and "extreme" processed gelose 80 starch samples are displayed both "dry" and in excess water. In agreement with previous studies,[22] on adding water, the peak associated with the 9 nm d-spacing characteristic of native starches ($q \sim 0.07$ A^{-1}) appears. With the side-chain liquid-crystalline model in mind, the reason why this peak is only observed upon the addition of water could be ascribed to the change from a glassy nematic state (dry starch) to a lamellar smectic structure with highly mobile backbone and spacers (hydrated starch).[23] Another peak is observed in the native starch

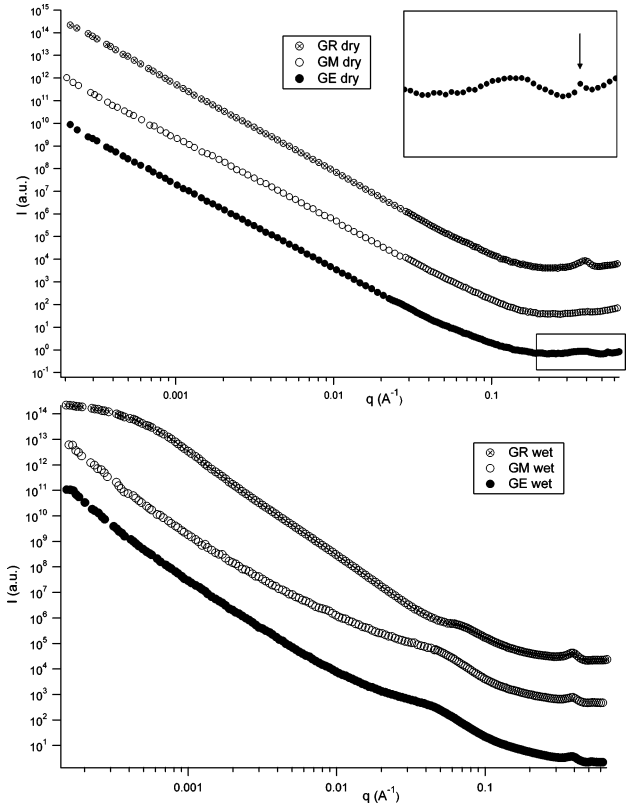

Figure 1. Effect of processing on USAXS/SAXS data: GR (gelose 80 raw), GM (gelose 80 "mild" processed), and GE (gelose 80 "extreme" processed). Upper graph: "dry" starch samples (arrow in inset points at the reflection from V-type crystallinity). Lower graph: excess water experiments. Data have been offset for clarity.

curve at $q \sim 0.4$ A^{-1} which corresponds to the 100 interhelix reflection typical of the B-type crystallinity.[7]

Surprisingly, while it seems that gelatinization is complete in the mild processed sample, the peak from the 100 reflection is still present in the "extreme" processed material. The reason is that, although the temperature and shear rate used were higher for the latter sample, its moisture content was just of 35%. It has been observed that when the concentration of starch is 55% w/w or higher, there is insufficient water in the amorphous phase to initiate the cooperative melting of crystallites, and therefore, a higher temperature will be needed to completely disrupt the structure.[24] This peak has, however, a lower intensity, and it is broader than in native starch, reflecting the crystalline disruption taking place during extrusion. Furthermore, as a consequence of "extreme" processing, a new peak arises at $q \sim 0.55$ A^{-1}, which is related to Bragg distances of ~1.2 nm ($2\theta \sim 7.5°$) present in V-type X-ray patterns (see the inset in Figure 1). V-crystals of starch consist of the regular packing of ordered amylose single helices with a diameter of 1.3 and 1.36 nm for the dehydrated[25] and hydrated[26] forms, respectively. The formation of these single-amylose helices upon extrusion has been described previously,[27,28] but it is evident that such a morphology is a function of temperature and shear rate as, in this work, it has only been observed for the "extreme" processed and not for the "mild" processed samples.

When the powdered starch samples at low moisture content are packed in a capillary for SAXS, the large density difference at the interface between the granules and the gaps between them is more significant than the density differences within the granules, and therefore, the scattering from low-moisture starches is mainly due to surface fractal structures (slopes close to −4).[29] As a result, the scattering data presented for the "dry" samples can be well described by a "power law plus Gaussian" function (see Figure 2):

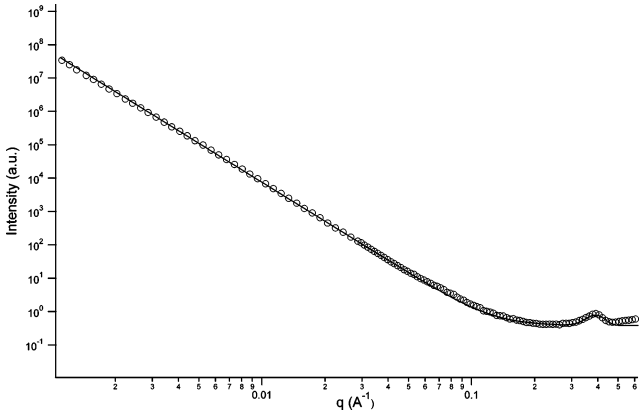

Figure 2. USAXS/SAXS curve for gelose 80 raw (dry powders). Experimental data (circle markers) fit to a "power law plus Gaussian" model (solid curve).

Table 1. Value of the Parameters Obtained by Fitting the Scattering Data of Undigested Dry High-Amylose Starch Samples to a "Power Law Plus Gaussian" Model (eq 1)

	power law exponent (δ)	height (I_0)	peak position (q_0)	width (B)
GR	3.878(4)	0.396(3)	0.387(1)	0.032(1)
GM	3.689(3)			
GE	3.599(4)	0.221(3)	0.375(1)	0.049(1)

$$I(q) = Aq^{-\delta} + I_0 \exp\left[-\frac{1}{2}\left(\frac{q - q_0}{B}\right)^2\right] + \text{Bkgd} \qquad (1)$$

From the value of the fitting parameters, information about the surface structure and the characteristic 100 reflection of B-type crystallinity can be obtained. The first term of the equation is the power law function, where A is the prefactor and δ is the power law exponent; the second term is the Gaussian function, where I_0 is the peak height, q_0 is its mean position, and B is the standard deviation (width of the peak). The values of these parameters for the high-amylose maize starch raw, and following "mild" and "extreme" processing are given in Table 1.

From this table it can be observed that the slope of the scattering curve decreases upon processing. In fact, very few experimental systems are found to follow the expressions corresponding to Porod's ideal two-phase system, the major causes of deviations from q^{-4} behavior being fluctuations in electron density within a phase, interfacial roughness, interfacial curvature, and gradual electron density variation across the interface.[30] The positive deviations from Porod's law observed here are due to increased surface roughness caused by the extrusion process; this is demonstrated later on, but on a larger scale, with the SEM images. Regarding the 100 reflection from B-type crystallinity ($q \sim 0.4$ A^{-1}), the partial gelatinization that takes place during extrusion is reflected in the decreased peak height and increased peak width. As mentioned before, in the "mild" extruded sample this peak disappears. A displacement of the reflection toward lower q after "extreme" extrusion is also observed.

In the excess water experiments, the scattering pattern is dominated by the scattering density difference between the amorphous and the crystalline regions inside the granules, as water fills the gaps between the starch granules and is absorbed

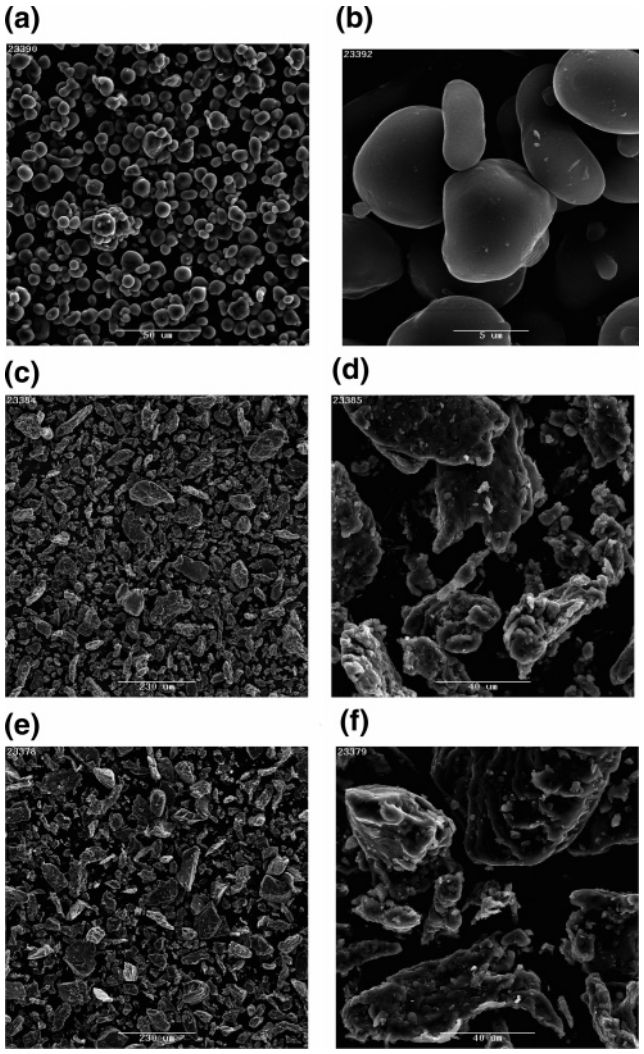

Figure 3. Scanning electron micrographs of high-amylose native starch (a → magnification 500×; b → magnification 4500×) extruded under "mild" conditions (c → magnification 100×; d → magnification 700×) and extruded under "extreme" conditions (e → magnification 100×; f → magnification 700×).

by the amorphous regions causing swelling (see Figure 1). The first remarkable feature in this figure is that the 100 reflection of the B-type crystallinity is present again in both extruded samples and the peak is comparable in shape and size to that of the native material. Upon extrusion, both under "mild" and "extreme" conditions, the 9 nm spacing is lost. Instead, a "shoulder", indicative of molecular order, is observed in both curves, so it seems that upon addition of water to the processed starch, retrogradation takes place quite quickly. In comparison with the 9 nm peak observed in the native starch, those shoulders are broader and less defined, indicating a broad distribution of molecular organization in this first stage of retrogradation. Models developed by Cameron and Donald[31] for fitting small-angle scattering data of raw starches were found to be unsuitable for processed starches, as the original structure is substantially disrupted during gelatinization. Alternative approaches for fitting of the data are being pursued. To enable comparison, a simple "power law plus two-phase nonparticulate system" model is used here (see below).

Scanning electron micrographs of the native and extruded starch are presented in Figure 3. Most of the high-amylose starch granules are rounded in shape with a smooth surface (Figure 3, parts a and b). However, and as observed previously in other high-amylose maize starches, some of the granules are elongated, filamentous structures with multiple growth directions, which have been suggested to be due to aberrant initiation of new granules.[32] The size of these native granules ranges from 5 to 10 μm.

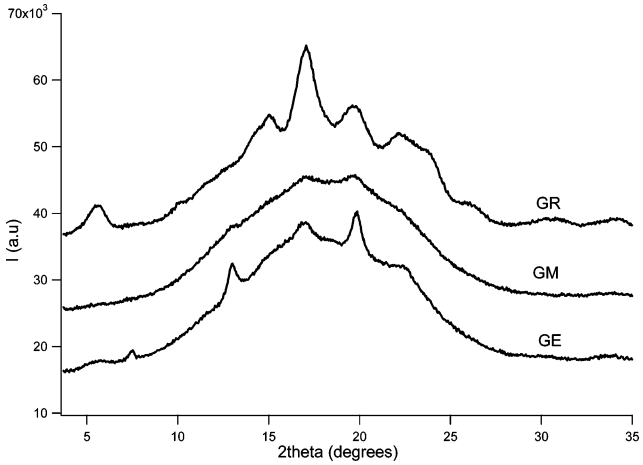

Figure 4. Effect of processing on X-ray diffraction data: GR (gelose 80 raw), GM (gelose 80 "mild" processed), and GE (gelose 80 "extreme" processed). Data have been offset for clarity.

After extrusion the granular structure is completely lost and both in the "mild" and "extreme" extruded starches, irregularly shaped, bigger, and mostly amorphous particles are left (Figure 3c−f). The size distribution of these processed freeze-dried starch particles is also broader, ranging from small particles of a few micrometers to aggregates of more than 100 μm. In the higher magnification micrographs, an increased surface roughness is observed in comparison with the smoother surface of the native granules.

To gain further information on the structural changes taking place as a consequence of extrusion, XRD patterns of the powdered starches were collected. As can be observed in Figure 4, native gelose 80 displays a typical B-type crystalline structure with a main peak around $2\theta \sim 17°$. The peak at ~5.5° is considered a fingerprint of this polymorph, and three other maxima are present around 22.2°, 23.7°, and 26.2°. A peak at $2\theta \sim 19.8°$ can also be observed which has been previously observed in high-amylose starches and is normally ascribed to amylose−lipid complexes.[33,34] However, the X-ray V-pattern does not always imply that a fatty acid is present within the single-amylose helix.[35]

"Mild" extrusion conditions lead to an almost fully gelatinized sample as indicated by the loss of Bragg peaks, and this is in agreement with the SAXS data. In contrast, for the "extreme" processed samples, not only are some of the reflections from the B-type crystallinity maintained after extrusion but also new reflections arise at $2\theta = 7.5°$ and 13°, which correspond to amylose single helices organized in a V-type crystallinity type. As previously mentioned, it seems that the formation of amylose single helices is favored under high-shear extrusion conditions.

Effect of Digestion on the Structure of Native and Extruded High-Amylose Starches. The RS fractions obtained after digestion of native and extruded high-amylose maize starch were also analyzed with USAXS and SAXS as received (freeze-dried powders) and after adding excess water (Figure 5).

In the case of the "dry" scattering patterns, significant changes were observed. After enzymatic hydrolysis of the native starch, the 100 reflection of B-type crystallinity ($q \sim 0.4$ Å^{-1}) cannot

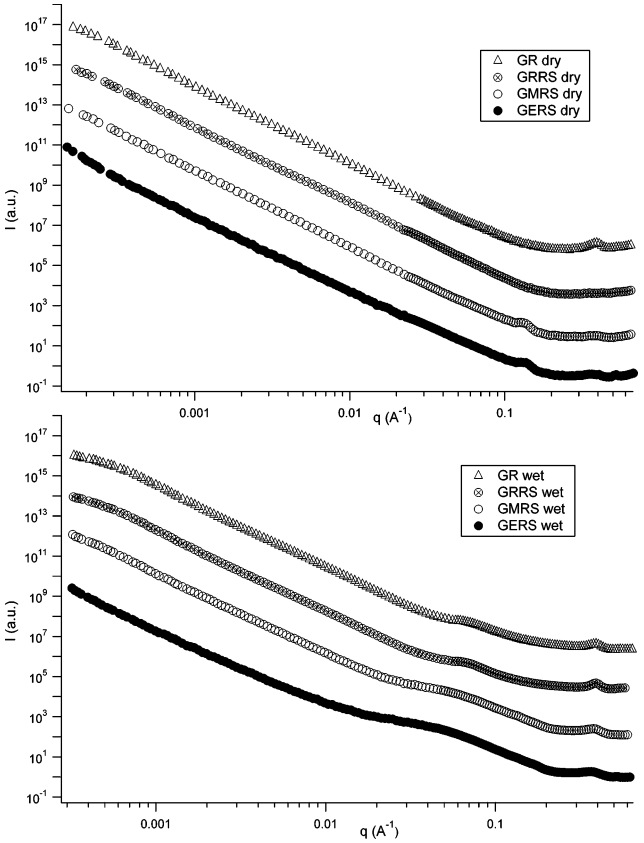

Figure 5. Effect of digestion on USAXS/SAXS data: GR (gelose 80 raw), GRRS (resistant starch fraction of gelose 80 raw), GMRS (resistant starch fraction of gelose 80 "mild" processed), and GERS (resistant starch fraction of gelose 80 "extreme" processed). Upper graph: "dry" starch samples. Lower graph: excess water experiments. Data have been offset for clarity.

be seen, pointing out that apart from hydrolyzing the amorphous areas, some disruption of the crystallinity occurs during digestion.

On the other hand, in the dry RS fractions of the extruded gelose 80, a new peak at $q \sim 0.137$ A^{-1} appears, which is related to Bragg distances of ~5 nm and may indicate that a new level of molecular organization has been established in the processed samples during α-amylase hydrolysis. This is the first time that this characteristic peak has been observed, which could be due to the fact that these experiments were carried out on the dry starch, while in previous work dealing with RS[13] SAXS analysis was performed on hydrated starch samples. A better resolution of the 100 reflection is also observed in the extruded samples after digestion.

It has been observed that enzymatic hydrolysis is able to induce retrogradation with crystal growth and formation being encouraged.[36] However, the amount of retrogradation during digestion will very likely be dependent on the degree of crystallinity and crystal perfection of the starting material, i.e., the higher the molecular order, the lower the impact of enzymatic hydrolysis in those materials. As a consequence of extrusion, as seen before, the high-amylose starches are, at least, partially gelatinized, and therefore, those samples are capable of undergoing some kind of reordering during the digestion process. As the enzyme hydrolyzes the bonds between the glucose molecules, the starch net is disrupted, decreasing the viscosity[37] and thus favoring the reorganization of the chains as a consequence of the increased molecular mobility.

How these chains reorder from the gelatinized state is still not clear. Cagiao et al.[38] studied the retrogradation of injection-molded potato starch during annealing and determined that the first crystals appearing from the gelatinized structure are the largest ones, and with increasing temperature, a decrease in crystal size takes place until a value of 6 nm is reached. This decrease in L has been ascribed to the growth of thin crystals inside or outside the lamellar stacks.

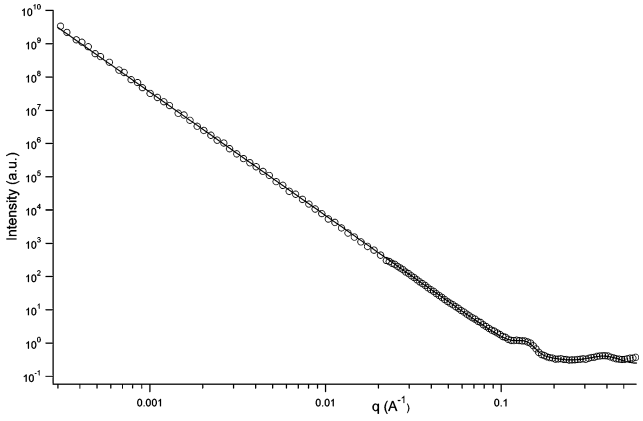

Figure 6. USAXS/SAXS curve for the resistant starch fraction of gelose 80 "mild" processed (dry powders). Experimental data (circle markers) fit by a "power law plus two Gaussian" model (solid curve).

The long period observed in the present study for the RS fractions of extruded high-amylose starch (~5 nm) is smaller than what has been previously reported, and it has only been detected in the dry experiments' curves. The molecular weight of gelose 80 has been observed to decrease to 7 kDa after processing and digestion (results not shown), which correspond to chain lengths of 30−40 glucoses. Considering how the molecules of starch crystallize in single and double helices,[39] having 6 and 12 glucose units per helix turn, respectively, it could be stated, as a first hypothesis, that this length corresponds to the most probable thickness of crystals present in the dry RS fractions of high-amylose maize starch.

In order to fit the curves from the dry RS fractions, a "power law plus two Gaussian" model was used with the aim of also describing the new structural peak (see Figure 6). The values of the fitting parameters are displayed in Table 2.

Digestion of native gelose 80 results in a slight decrease in the absolute value of the slope of the USAXS/SAXS curves (see the power law exponent in Table 2), which, as expected, indicates a rougher surface of the remaining starch granules after digestion. In contrast, the absolute values of the slopes for the RS fractions from the processed materials are slightly increased (see the power law exponents in Table 1 for comparison).

The fitting parameters that describe the 100 reflection related with B-type crystallinity in starches point to the disappearance of this peak for the RS fraction of native starch and to the formation of this reflection during digestion of the "mild" processed starch.

Addition of water induces the retrogradation of starch, as mentioned before (see the lower graph in Figure 5). This is primarily reflected by the increase in the reflection at $q \sim 0.4$ Å^{-1} for every RS curve.

The raw sample, after digestion, still shows the 9 nm peak, meaning that the original repetitive crystalline pattern does not substantially change during α-amylolysis of native granules and, although as previously mentioned the crystallinity is somehow disrupted during the digestion process, the addition of water seems to cause retrogradation which leads to a structure similar to that of the original.

Apparently, from these results, the structure of the RS fractions of the processed materials is substantially different to

Table 2. Value of the Parameters Obtained by Fitting the Scattering Data of the Dry Gelose 80 Resistant Starch Fractions to a "Power Law Plus Two Gaussian" Model

		"5 nm" peak			100 reflection		
	power law exponent (δ)	height (I_0)	peak position (q_0)	width (B)	height (I_0)	peak position (q_0)	width (B)
GRRS	3.758(5)						
GMRS	3.710(4)	0.504(9)	0.136(1)	0.014(1)	0.152(2)	0.387(1)	0.070(1)
GERS	3.617(1)	0.617(9)	0.137(1)	0.011(1)	0.135(4)	0.368(1)	0.061(2)

that of the native starch. While in the native granules the crystals are perfectly arranged into lamellar structures, after gelatinization and digestion the structure is completely different, and upon addition of water to the RS fractions of the processed starches the peak at $q \sim 0.13$ Å^{-1}, observed in the dry RS fractions of the extruded starch, is no longer seen. Instead, a shoulder similar to those observed in the undigested samples is present. To the best of our knowledge, there is only one paper published in which the structure of RS has been investigated with SAXS.[40] The experiments in the previous work were carried out with starch suspensions, i.e., in excess water, and in the SAXS curves a "shoulder" at low q was observed, similar to those displayed in Figures 1 and 5 for the processed and hydrated starch samples, which the authors attributed to the formation of a periodic structure. In common with the mentioned work, for fitting the USAXS/SAXS data of the processed samples with water (both before digestion and the RS fractions), a "two-phase nonparticulate system" model has been used, but to which we have added a power law function to account for the vastly extended q-range available:

$$I(q) = Aq^{-\delta} + \left[\frac{BX_c(1 - X_c)\epsilon^3}{(1 + q^2\epsilon^2)^2}\right] \qquad (2)$$

Again, the first term of the equation corresponds to the "power law" model which provides the slope of the USAXS curves represented on a logarithmic scale, and the second term is the "two-phase nonparticulate system" model where X_c is the degree of crystallinity (%), ϵ is the characteristic length of the system, and B is a prefactor that is proportional to the electron density contrast of the crystalline and amorphous phases.[40] The "two-phase nonparticulate" model illustrates a semicrystalline material formed by crystallites of various sizes distributed in an amorphous matrix.[41] Therefore, the characteristic length is calculated from the average thickness of the crystallites and the average thickness of the amorphous phase between the crystallites (see formula below).

Figure 7 shows, as an example, the fitting of this model to the RS fraction of gelose 80 extruded under "extreme" conditions.

The values of the fitting parameters for the extruded gelose 80 before and after digestion, used to fit the USAXS/SAXS curves of the starches in the presence of water, are displayed in Table 3.

From this table an increase in the absolute value of the power law exponent is observed in the RS fractions as well as an increase in the crystallinity content. However, whether retrogradation is higher in the presence of α-amylase cannot be confirmed, as after digestion we analyzed only the RS fraction, i.e., after removing the digested part which is thought to be mostly amorphous. It should also be noted that the crystallinity values are higher than those calculated from the XRD data (see below) in which the samples were analyzed dry. However, the different analytical methods used in the two techniques to determine the crystallinity precludes this, in itself, as sufficient evidence of retrogradation taking place in the presence of water. Regarding the characteristic length of the system, a different behavior is observed for the "mild" and "extreme" processed samples, with a decrease in the value for the former and no significant changes for the latter. In the "two-phase nonparticulate system" model, the characteristic length of the system is described as follows:

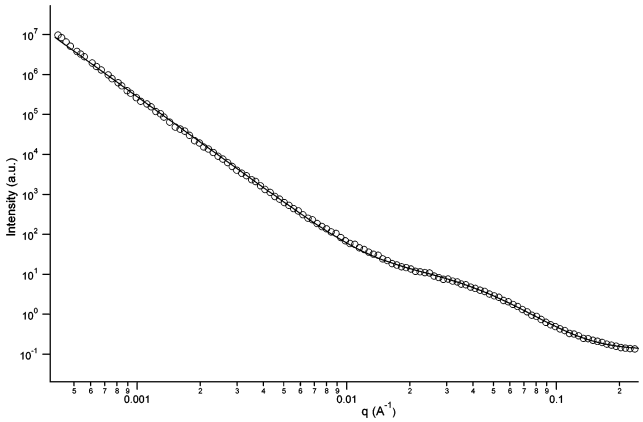

Figure 7. USAXS/SAXS curve for the resistant starch fraction of gelose 80 extruded under "extreme" conditions (excess water experiment). Experimental data (circle markers) fit to a "power law plus two-phase nonparticulate system" model (solid curve).

Table 3. Value of the Parameters Obtained by Fitting the Scattering Data of Processed Gelose 80 before and after Digestion to a "Power Law Plus Two-Phase Nonparticulate" Model (eq 2)[a]

		power law exponent (δ)	crystallinity (X_c)	characteristic length (ϵ)
mild processed	undigested	3.67(1)	0.17(1)	23.12(9)
	digested	3.99(1)	0.50(9)	17.09(9)
extreme processed	undigested	3.70(1)	0.23(1)	23.69(9)
	digested	3.78(1)	0.38(2)	23.95(9)

[a] Excess water experiments.

$$\frac{1}{\epsilon} = \frac{1}{\langle\epsilon_c\rangle} + \frac{1}{\langle\epsilon_a\rangle} \qquad (3)$$

where ϵ_c and ϵ_a are the average lengths of the crystallites and of the amorphous phase between the crystallites, respectively. These values, therefore, can be easily calculated using the crystallinity of the system:

$$\epsilon = (1 - \varphi)\langle\epsilon_c\rangle = \varphi\langle\epsilon_a\rangle \qquad (4)$$

Therefore, an increase in crystal thickness takes place during digestion, as deduced from the fitting of the curves, with ϵ_c increasing from ~28 to ~34 nm and from ~31 to ~39 nm for

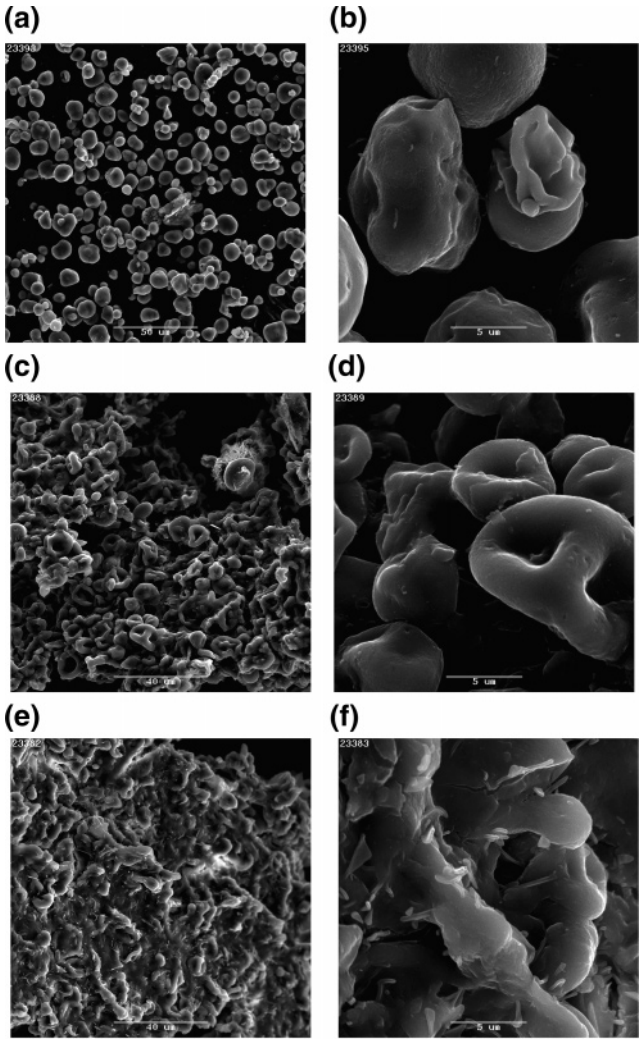

Figure 8. SEM images of the resistant starch fractions of high-amylose starch native (a → magnification 500×; b → magnification 4500×) extruded under "mild" conditions (c → magnification 700×; d → magnification 4500×) and extruded under "extreme" conditions (e → magnification 700×; f → magnification 4500×).

the mild and extreme processed samples, respectively. This seems reasonable taking into account that the crystals present in the RS fractions are due not only to the addition of water before the experiments but also to the crystallinity developed during the digestion process, in which water at higher temperature (~37 °C) during a long time (18 h) was involved.

Further substantiation of the retrogradation process taking place in the extruded samples during digestion was gained with SEM and XRD.

In Figure 8 the scanning electron photomicrographs of the different RS fractions are presented. The fraction left after digestion of native starch (Figure 8, parts a and b) has roughened surfaces, supporting the explanation for the decrease in the absolute value of the SAXS curves' slopes. SAXS and SEM are complementary methods useful to investigate different size ranges. However, in this case, it seems that digestion leads to an increased roughness both at the micrometer and at the nanometer scale. This feature has previously been observed after digestion of other starches.[42] In the lower magnification micrograph, apart from intact granules, there are some others which have been partially digested, showing circular erosion areas over the surface. A few granules in the RSII fraction (as shown in Figure 8b) were extensively eroded over the entire surface.

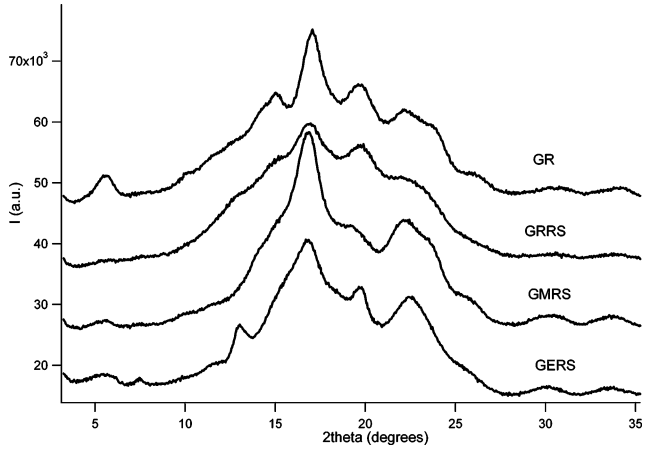

Figure 9. Effect of digestion on X-ray diffraction data: GR (gelose 80 raw), GRRS (resistant starch fraction of gelose 80 raw), GMRS (resistant starch fraction of gelose 80 "mild" processed), and GERS (resistant starch fraction of gelose 80 "extreme" processed). Data have been offset for clarity.

After digestion of the processed high-amylose starch a slight increase in the absolute value of the slope in the USAXS/SAXS curves is noticeable, and over the larger size range available with SEM, smoother surfaces of the RS fractions are clearly observed (see Figure 8, parts d and f).

Digestion of "mild" extruded starch leaves behind disc-shaped particles with depressions in the center. Similar shapes have been observed previously in starches treated with citric acid, in which some of the granules were doughnut-shaped with their outer sides drawn inward,[43] and in slowly cooled starch solutions prepared by steam jet cooking, in which high-amylose starches yielded crystalline disc-shaped particles, with a mean diameter of 13.3 μm and depressions in the center.[44] The formation of the latter spherocrystalline particles was ascribed to the crystallization of helical inclusion complexes formed from amylose and the native lipid material present in cereal starch granules. Although the particles seen in Figure 8, parts c and d, cannot be related to any of the previous work (neither citric acid was involved in digestion, nor was a V-type crystallinity observed in this sample as will be shown below), it is quite obvious that some kind of ordering has taken place during digestion.

Similar statements can be made regarding the micrographs of the "extreme" extruded samples after digestion (Figure 8, parts e and f). Although the morphology is quite different to that observed for the "mild" extruded high-amylose starch, a more organized structure of the "extreme" processed sample can be visualized after digestion. In this case, within the bulk structure, smaller needle-like particles are present, which could be due to some kind of structural organization formed during extrusion under high temperature and high shear rate conditions that is able to resist digestion.

In Figure 9, the diffractograms of the RS fractions have been plotted together with the diffractogram of the raw material for comparison. In common with the other techniques used, a decrease in the crystallinity is observed in the native starch after digestion, reflected in the lower intensity of the crystalline reflections and even in the disappearance of some diffraction peaks. In contrast, a considerable improvement in molecular order takes place in the extruded samples during digestion proving that retrogradation is favored in these processed starches. In some studies dealing with RSIII, the processing method used was autoclaving, and XRD patterns typical of B-type crystallinity were obtained.[45] The same crystal polymorphs were found after digestion of starch gels.[46]

Table 4. Degree of Crystallinity (X_c, %) of the Different Samples Calculated from the X-ray Diffraction Data

	GR	GM	GE
X_c before digestion (%)	17.3	2.5	5.4
X_c after digestion (%)	6.8	22.5	23.5

The crystalline morphologies of the RSIII fractions obtained in this study are rather different from the high-amylose native structure. The "mild" processed high-amylose starches, after digestion, exhibit a diffraction pattern similar to that of the B-type, but the reflections at 5° and 15° are very weak. On the other hand, the "extreme" processed starches show mixed C- and V-type patterns. Previous studies on high-amylose maize starch with different additives showed that RS obtained from extruded samples displayed V-type crystallinity.[47] Whether these reflections are a consequence of amylose−lipid complexes is currently under investigation. It is worth mentioning that the reflection at $2\theta \sim 20°$, which is normally attributed to amylose−lipid complexes, remains after the digestion of the different samples. Nevertheless, the intensity of this reflection is very weak in the case of the "mild" processed samples, slightly decreases in the native starches, and remains almost the same in the "extreme" processed ones. Therefore, the processing conditions seem to be a determinant in the resistance to digestion of this specific fraction of starch which is of primary importance for gut health.

In Table 4, the crystallinity values for the different samples before and after digestion are displayed. During extrusion starch undergoes a melting process, which results in a partial loss of the crystallinity present in the native material. However, after digestion of the extruded samples, surprisingly, the crystallinity values attained are higher than those of the native materials.

Digestion of the "raw" starches, on the other hand, leads to a decrease in the crystalline order. This result contrasts with previous observations in which the amorphous parts of the starch granules were preferentially etched during digestion, because in that case, the crystallinity should be higher than that of the native material. Probably during the first stages of digestion the softer parts of the granule are mainly hydrolyzed, but after 18 h the original crystalline structure is substantially affected as demonstrated by the XRD results. This implies that the RSII fractions left are determined, not only by the initial crystallinity of starch, but also by the organization of the crystals within the starch granule, as this latter factor will considerably affect the kinetics of digestion.

In a subsequent publication, we will correlate the supramolecular order, as identified here, with the molecular conformation of the starch polymers and their thermal characteristics.[48]

Conclusions

In this work the structural changes of a commercial high-amylose maize starch as a consequence of extrusion and digestion have been described. It has been observed that depending on the extrusion conditions used, different degrees of gelatinization are obtained, as well as different RS fraction morphologies. "Mild" processing of the starches (50% moisture content, 100 °C, and 150 s^{-1} shear rate) resulted in almost fully gelatinized starches, and during digestion, a B-type crystallinity was developed. In contrast, "extreme" processing (35% moisture content, 140 °C, and 750 s^{-1} shear rate) led to the formation of single-amylose helices which resisted the digestion process and to a lower degree of gelatinization, probably due to the low-humidity conditions used. The RS fraction left after digestion of the latter materials showed a completely different morphology which consisted of a mixture of C-type and V-type crystal unit cells.

Water has been observed to strongly influence the structure of starch, causing retrogradation in processed starches and even changing the RS structure, as observed by SAXS. In the RS fractions obtained from the processed starches a peak at ∼5 nm in the SAXS curves, reflecting some kind of repetitive characteristic length, was observed when the experiments were carried out in dry conditions, but after adding water, the USAXS/SAXS curves displayed a broad shoulder, extended over a range of q-values, indicating a less defined structure. This work shows that the resistance to digestion is not due to a specific structure, but it is related to the competition between the kinetics of retrogradation and enzymatic hydrolysis during digestion.

Acknowledgment. The authors thank Surjani Uthayakumaran, Udayasika Piyasiri, Hélène Chanvrier, and Tony Burrows from Food Science Australia for the preparation of the samples and Professor M. Gidley for fruitful discussions. Jan Ilavsky is also acknowledged for kindly performing the USAXS experiments.

References and Notes

(1) Topping, D. L.; Clifton, P. M. *Physiol. Rev.* **2001**, *81*, 1031−1064.
(2) Englyst, H. N.; Cummings, J. H. *Am. J. Clin. Nutr.* **1987**, *45*, 423−431.
(3) Tang, H.; Mitsunaga, T.; Kawamura, Y. *Carbohydr. Polym.* **2006**, *63*, 555−560.
(4) Waigh, T. A.; Perry, P.; Riekel, C.; Gidley, M. J.; Donald, A. M. *Macromolecules* **1998**, *31*, 7980−7984.
(5) Hizukuri, S.; Kaneko, T.; Takeda, Y. *Biochim. Biophys. Acta* **1983**, *760*, 188−191.
(6) Hizukuri, S. *Carbohydr. Res.* **1985**, *141*, 295−306.
(7) Sarko, A.; Wu, H. C. H. *Starch/Staerke* **1978**, *30*, 73−78.
(8) Imberty, A.; Perez, S. *Biopolymers* **1988**, *27*, 1205−1221.
(9) Imberty, A.; Chanzy, H.; Perez, S. *J. Mol. Biol.* **1988**, *201*, 365−378.
(10) Sevenou, O.; Hill, S. E.; Farhat, I. A.; Mitchell, J. R. *Int. J. Biol. Macromol.* **2002**, *31*, 79−85.
(11) Chanzy, H.; Putaux, J. L.; Dupeyre, D.; Davies, R.; Burghammer, M.; Montanari, S.; Riekel, C. *J. Struct. Biol.* **2006**, *154*, 100−110.
(12) Gidley, M. J.; Cooke, D.; Darke, A. H.; Hoffmann, R. A.; Russell, A. L.; Greenwell, P. *Carbohydr. Polym.* **1995**, *28*, 23−31.
(13) Shamai, K.; Bianco-Peled, H.; Shimoni, E. *Carbohydr. Polym.* **2003**, *54*, 363−369.
(14) Sievert, D.; Czuchajowska, Z.; Pomeranz, Y. *Cereal Chem.* **1991**, *68*, 86−91.
(15) Lehmann, U.; Rössler, C.; Schmiedl, D.; Jacobasch, G. *Nahrung* **2003**, *47*, 60−63.
(16) Pohu, A.; Putaux, J. L.; Planchot, V.; Colonna, P.; Buleon, A. *Biomacromolecules* **2004**, *5*, 119−125.
(17) Shin, S.; Byun, J.; Park, K. H.; Moon, T. W. *Cereal Chem.* **2004**, *81*, 194−198.
(18) Chung, H. J.; Lim, S. T. *Food Hydrocolloids* **2003**, *17*, 855−861.
(19) Muir, J.; Birkett, A.; Brown, I.; Jones, G.; O'Dea, K. *Am. J. Clin. Nutr.* **1995**, *61*, 82−89.
(20) Lake, J. A. *Acta Crystallogr.* **1967**, *23*, 191−194.
(21) Long, G. G.; Jemian, P. R.; Weertman, J. R.; Black, D. R.; Burdette, H. E.; Spal, R. *J. Appl. Crystallogr.* **1991**, *24*, 30−37.
(22) Cameron, R. E.; Donald, A. M. *Carbohydr. Res.* **1993**, *244*, 225−236.
(23) Waigh, T. A.; Kato, K. L.; Donald, A. M.; Gidley, M. J.; Clarke, C. J.; Riekel, C. *Starch/Staerke* **2000**, *52*, 450−460.
(24) Bernazzani, P.; Chapados, C.; Delmas, G. *Biopolymers* **2001**, *58*, 305−318.
(25) Murphy, V. G.; Zaslow, B.; French, A. D. *Biopolymers* **1975**, *14*, 1487−1501.
(26) Brisson, J.; Chanzy, H.; Winter, W. T. *Int. J. Biol. Macromol.* **1991**, *13*, 31−39.

(27) Cagiao, M. E.; Bayer, R. K.; Rueda, D. R.; Balta Calleja, F. J. *J. Appl. Polym. Sci.* **2003**, *88*, 17−27.
(28) Bindzus, W.; Livings, S. J.; Gloria-Hernandez, H.; Fayard, G.; van Lengerich, B.; Meuser, F. *Starch/Staerke* **2002**, *54*, 393−400.
(29) Suzuki, T.; Chiba, A.; Yano, T. *Carbohydr. Polym.* **1997**, *34*, 357−363.
(30) Foster, M. K. *Crit. Rev. Anal. Chem.* **1993**, *24*, 179−241.
(31) Cameron, R. E.; Donald, A. M. *Polymer* **1992**, *33*, 2628−2635.
(32) Glaring, M. A.; Koch, C. B.; Blennow, A. *Biomacromolecules* **2006**, *7*, 2310−2320.
(33) Vermeylen, R.; Goderis, B.; Reynaers, H.; Delcour, J. A. *Biomacromolecules* **2004**, *5*, 1775−1786.
(34) Le Bail, P.; Bizot, H.; Ollivon, M.; Seller, G.; Bourgaux, C.; Buleon, A. *Biopolymers* **1999**, *50*, 99−110.
(35) Godet, M. C.; Buleon, A.; Tran, V.; Colonna, P. *Carbohydr. Polym.* **1993**, *21*, 91−95.
(36) Cairns, P.; Sun, L.; Morris, V. J.; Ring, S. G. *J. Cereal Sci.* **1995**, *21*, 37−47.
(37) Hoebler, C.; Karinthi, A.; Devaux, M. F.; Guillon, F.; Gallant, D. J. G.; Bouchet, B.; Melegari, C.; Barry, J. L. *Br. J. Nutr.* **1998**, *80*, 429−436.
(38) Cagiao, M. E.; Rueda, D. R.; Bayer, R. K.; Balta Calleja, F. J. *J. Appl. Polym. Sci.* **2004**, *93*, 301−309.
(39) Bayer, R. K.; Balta-Calleja, F. J. *J. Macromol. Sci., Phys.* **2005**, *44*, 471−479.
(40) Shamai, K.; Shimoni, E.; Bianco-Peled, H. *Biomacromolecules* **2004**, *5*, 219−223.
(41) Balta-Calleja, F. J.; Vonk, C. G. In *Polymer Science Library 8. X-ray Scattering of Synthetic Polymers*; Jenkins, A. D., Ed.; Elsevier Science Publishers B. V.: New York, 1989.
(42) Hoover, R.; Manuel, H. *Food Chem.* **1995**, *53*, 275−284.
(43) Xie, X.; Liu, Q.; Cui, S. W. *Food Res. Int.* **2006**, *39*, 332−341.
(44) Fanta, G. F.; Felker, F. C.; Shogren, R. L. *Carbohydr. Polym.* **2002**, *48*, 161−170.
(45) Mun, S. H.; Shin, M. *Food Chem.* **2006**, *96*, 115−121.
(46) Cairns, P.; Morris, V. J.; Botham, R. L.; Ring, S. G. *J. Cereal Sci.* **1996**, *23*, 265−275.
(47) Adamu, B. O. A. *Starch/Staerke* **2001**, *53*, 582−591.
(48) Gidley, M. J.; Flanagan, B. M.; Shrestha, A.; Lopez Rubio, A.; Gilbert, E. P.; Htoon, A.; Chanvrier, H.; Uthayakumaran, S.; Lillford, P. J.; Zhou, X. K.; Bird, A. R.; Topping, D. L. *Asia Pac. J. Clin. Nutr.*, in press.

BM061124S